A new time-dependent analytic compact model for radiation-induced photocurrent in epitaxial structures

Jason C. Verley*, Eric R. Keiter,
Charles E. Hembree, Carl L. Axness (ret.)
Sandia National Laboratories
Albuquerque, New Mexico, USA
*jcverle@sandia.gov

Bert Kerr
Mathematics Department
New Mexico Institute of Mining and Technology
Socorro, New Mexico, USA

***Abstract*—Photocurrent generated by ionizing radiation represents a threat to microelectronics in radiation environments. Circuit simulation tools that employ compact models for individual electrical components (SPICE, *e.g.*) are often used to analyze these threats. Historically, many photocurrent compact models have suffered from accuracy issues due to the use of empirical assumptions, or physical approximations with limited validity. In this paper, an analytic model is developed for epitaxial diode structures that have a heavily-doped sub-collector. The analytic model is compared with both numerical TCAD calculations and the compact model described in reference [1]. The new analytic model compares well against TCAD over a wide range of operating conditions, and is shown to be superior to the older compact model [1]. The methods put forth in this paper could also be applied to model devices with similar physics, such as photonic and power devices.**

I. Introduction

The development of compact models that can simulate the excess carrier dynamics in undepleted semiconductor regions is important for many applications, including photonic and power devices. One application of interest is the calculation of photocurrent due to the uniform internal carrier generation in a device caused by ionizing radiation. Previous radiation-generated photocurrent compact models (*e.g.*, [1]) have been implemented in circuit codes such as SPICE and Xyce [2] with some success. However, those compact models have often applied empirical assumptions, or physical approximations with limited validity. As a result, the calibrations for many models can fail if applied to multiple time scales.

An improved photocurrent model for *pn*-type structures [3], which relied on fewer assumptions and used analytic solutions, addressed these calibration problems. In this work, the mathematical formulation presented in [3] is extended to include highly doped sub-collectors—a performance-enhancing feature of many devices. The model compares favorably to TCAD, and improves over an older compact model [1] for a hypothetical BJT with an $npnn^+$ sub-collector structure.

The analytic model presented here could be adapted to many situations concerning the movement of excess carriers in a non-depletion region of a device. The photogeneration could be optical, which applies to many kinds of optical sensors and photovoltaics or, the excess carriers could be due to some kind of injection, which is common in power devices.

II. Background

The transport behavior of excess carriers in semiconductors is often described using the well-known drift-diffusion equations [4], which are commonly used in device, *i.e.*, TCAD, simulations. However, these equations are not amenable to exact analytic mathematical techniques, so many photocurrent compact models (*e.g.*, [1], [5]) use the ambipolar diffusion equation (ADE) to model the behavior of excess carriers in the undepleted regions of a device.

The ADE is derived from the drift-diffusion equations using two approximations [4]. The first is the electrical neutrality, or charge balance approximation, which states that the excess electron and hole densities are equal across the entire domain. The second approximation is the congruence assumption, where the flux of electrons and holes out of any region must be equal. The resulting ADE is given by

$$\frac{\partial u}{\partial t} = D_a \nabla^2 u - \mu_a \mathbf{E} \cdot \nabla u - \frac{u}{\tau} + g \qquad (1)$$

where u is the excess carrier density (electrons or holes), D_a is the ambipolar diffusion constant, μ_a is the ambipolar mobility, τ is the carrier lifetime, g is the creation rate for electron-hole pairs, and $\mathbf{E}$ is the electric field.

In many cases, photocurrent-producing structures—such as reverse-biased *p-n* junctions (the base-collector of a BJT, e.g.), and the drain-body regions of MOSFETs—are constructed with epitaxial layers. Since epitaxial structures regions lend themselves to analysis by one-dimensional models, we restrict the ADE to one dimension (though our method can be extended to two or three dimensions for simple geometries). We also assume a uniform depletion region and negligible electric fields in the undepleted regions of the device.

The only analytic ADE solution for photocurrent in a sub-collector that we have found is by Long, Florian and Casey [5]. However, to simplify their analysis, they assumed, in addition to our assumptions, that the sub-collector is infinite; and they solved the problem analytically only for steady-state conditions. The photocurrent compact model by Fjeldly, *et al.* [1] also purports to treat the sub-collector, but not through an ADE solution. It makes the assumption that photocurrent collection from the sub-collector is limited to one diffusion length from the boundary.

Our derivation focuses on the undepleted nn^+ portion of a device. (Note that, while we examine nn^+ doping in this

978-1-4673-5736-4/13/$31.00 ©2013 IEEE

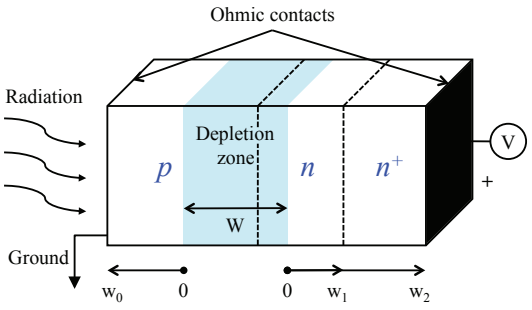

Fig. 1. Reverse-biased 1D abrupt junction pnn^+ diode under irradiation

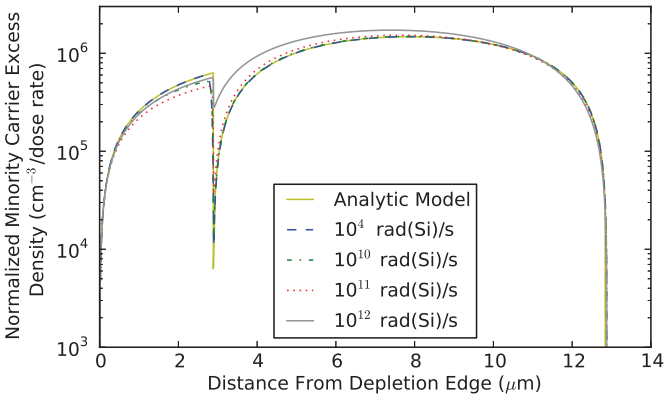

Fig. 2. Normalized (with respect to dose rate) steady-state excess minority carrier density for an irradiated nn^+ region as a function of position. The right depletion edge in the pnn^+ diode (Figure 1) would correspond to $x = 0$ in the figure. The densities with dose rate labels are simulated with TCAD.

work, pp^+ doping follows the same mathematics, but with a simple sign change.) Similar to previous work [3], [6], we use the finite Fourier transform technique [7] to solve the 1D ADE and describe the carrier dynamics in the unbiased nn^+ sub-component of an epitaxial device experiencing a radiation transient.

III. Mathematical Development

A detailed description of the mathematics can be found in [8], so only a brief overview will be given here. The device geometry is shown in Figure 1. For a reverse-biased 1D pnn^+ diode, the total photocurrent can be written as the sum of the photocurrent generated in each region, $J_{total} = J_n + J_{depl} + J_{pp}$ (the subscripts correspond to the minority carriers in each region, with pp referring to the combined collector/sub-collector region). Formulas for the photocurrent J_n and J_{depl} are already known, and may be found in [3]. The carrier dynamics in the undepleted nn^+ region are determined by using the finite Fourier transform method [7], [8] to solve the ADE in the two respective regions. The ADE (with $E = 0$) is given by

$$u_t = D_i u_{xx} - \frac{1}{\tau_i} u + g\,(t) \tag{2}$$

where $i = 1$ in the *n*-type region, and $i = 2$ in the sub-collector (n^+) region. D_1 and D_2 are the ambipolar diffusion coefficients, and τ_1 and τ_2 are the carrier lifetimes in the respective regions.

Dirichlet boundary conditions are assumed for the external boundaries. Physically, this is interpreted as perfect surface recombination conditions at the contact (on the right of the n^+ region), and that the holes entering the depletion zone from the *n*-type region are all converted to photocurrent. The interface boundary conditions (following those in [5]) require that the excess carrier current be continuous through the nn^+ interface,

$$D_1 \frac{\partial u}{\partial x}\bigg|_{x=w_1^-} = D_2 \frac{\partial u}{\partial x}\bigg|_{x=w_1^+} \tag{3}$$

and that the ratio of the excess carrier density on each side of the interface remains fixed at a value dictated by the ratio of the majority carrier concentrations, N_1 and N_2,

$$N_1 u\left(w_1^-, t\right) = N_2 u\left(w_1^+, t\right) \tag{4}$$

The two composite layers within the region, coupled with the interface boundary conditions, produce a sequence of piecewise continuous eigenfunctions, in which the eigenvalues are given by a transcendental equation. The formula for the excess carrier density in the nn^+ region, with the initial condition $u\,(x, 0) = 0$, may be written as

$$u\,(x,t) = \sum_{n=1}^{\infty} w_n \int_0^t g\,(v)\, e^{-\lambda_n (t-v)} dv \frac{X_n\,(x)}{\|X_n\|^2} \tag{5}$$

The X_n are the eigenfunctions, the λ_n are the associated eigenvalues and $w_n = \langle 1 \cdot X_n(x) \rangle$. The associated photocurrent is given by

$$\begin{aligned} J_{pp}(t) &= qD_1 \frac{\partial u}{\partial x}\bigg|_{x=0} \\ &= qD_1 \sum_{n=1}^{\infty} w_n \int_0^t g\,(v)\, e^{-\lambda_n (t-v)} dv \frac{X_n'(0)}{\|X_n\|^2} \end{aligned} \tag{6}$$

where q is the elementary charge.

To optimize the efficiency of our compact model, we also simplified the series in equation (6) for the case when the generation function is given in the form of a discrete data set, by assuming the points define a piecewise linear $g\,(t)$. This enables us to easily analyze an arbitrarily-shaped generation function [8]. The relevant series converges quickly, with initial work indicating the series will typically require no more than a few tens of terms to converge.

IV. Code Comparison

While the ultimate test of the analytic sub-collector model will be comparison to experiments, this work focuses on validating the mathematical accuracy of the model as compared to TCAD or other compact models—especially the Fjeldly model [1]. Our initial comparisons involve the characteristics of just the nn^+ portion of a device. We then examine the simulated response of a hypothetical BJT to a radiation pulse, with the transistor situated in a realistic test circuit.

Figure 2 illustrates steady-state analytic and TCAD normalized excess minority carrier densities within an unbiased irradiated nn^+ doped silicon region. The TCAD excess carrier densities in the plot are normalized by the radiation dose

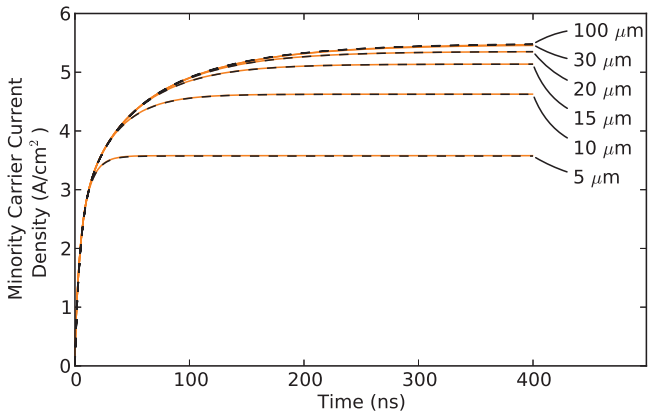

Fig. 3. Transient, normalized analytic and TCAD photocurrent densities for the nn^+ region as a function of the sub-collector thickness, for a long 10^9 rad(Si)/s irradiation. The TCAD results are plotted as dashed lines.

rate. Continuous radiation pulses with dose rates between 10^4 rad(Si)/s and 10^{12} rad(Si)/s were simulated, and the excess carrier densities are plotted 100 µs after pulse initiation, which is well after steady-state conditions were achieved. The TCAD simulations show that the dependence of the excess carrier density on the dose rate is approximately linear for dose rates less than 10^{10} rad(Si)/s, and are in close agreement with the analytic solution over this range. A (quasi-)discontinuity in the densities is evident at the nn^+ interface. In the TCAD simulations the feature is a consequence of the doping discontinuity; but no explicit boundary conditions are enforced at the interface. The discontinuity in the analytic solutions is due to the boundary conditions expressed in equations (3) and (4), and the consistency between the TCAD simulations and the analytic solution supports their use. Higher dose rates (high-level irradiations) in the TCAD solutions show an increase in the excess carrier density in the n^+ region, and a decrease in the excess carrier discontinuity at the nn^+ interface, thus indicating a breakdown of the assumptions inherent in the ADE. It is likely the difference in the minimum value of the interface carrier density is due to the mesh-based discretization of the TCAD calculation.

Figure 3 compares the analytic and simulated TCAD results for the minority carrier photocurrent densities from an nn^+ region for various thicknesses of the n^+ sub-collector. The radiation dose rate is 10^9 rad(Si)/s, and the sub-collector thickness is indicated on the right side of the figure. The analytic and TCAD plots essentially overlap in each case. It is apparent that, for the parameters and doping levels used in these nn^+ simulations, a significant amount of charge is collected from deep within the sub-collector (in the range of 20 µm–30 µm). Recall that the Fjeldly model [1] assumes photocurrent collection from the sub-collector only within one diffusion length. The diffusion length in this case is approximately 5 µm, which indicates that the Fjeldly assumption does not account for all of the delayed photocurrent contributions.

A comparison of the analytic model to the Fjeldly model and TCAD simulations is shown in Figure 4 for a hypothetical $npnn^+$ BJT. The transistor was simulated as part of a circuit that is representative of one used to test BJTs at radiation facilities. Specifically, the base and emitter are shorted together, and attached to ground via a 50 Ω resistor. The collector is attached to a 5 V bias. A sawtooth waveform was chosen to represent the radiation pulse, and is shown in Figure 4a. While the waveform is not physically realistic, the abrupt changes and smooth final decay provide a good exercise for the analytic model.

Recall one of the failures of previous photocurrent compact models was a loss of accuracy when they were used at time scales different from the time scale on which they were calibrated. To examine the robustness of the analytic model with regard to time scale variability, two additional simulations were run using the same pulse shape, but compressed to shorter time scales. The Fjeldly model was calibrated to the nominal time scale, matching that shown in Figure 4a. Also, the values of the minority carrier mobility and lifetime used in the analytic and TCAD models were matched to the Fjeldly model.

For the analytic model, the photocurrent from the BJT is the sum of the photocurrent computed by solving the ADE in each of the undepleted regions, along with the sum of the photocurrent from the two depletion zones. The photocurrent from the undepleted *p* and *n* regions were calculated using the photocurrent solution from [3]. The analytic current from the depleted regions was calculated using the expression, $J_{depl} = qg(t)W$. The depletion widths, W, were calculated from the standard abrupt *pn*-junction formula [4].

Figures 4b, 4c and 4d compare the analytic, Fjeldly and TCAD simulated current going through the 50 Ω resistor for the three different input pulse time scales. Figure 4b represents the nominal time scale, so the excellent agreement between the three solutions is expected. When the time scale of the pulse is compressed by a factor of 100, though, as in Figure 4c, the limitations of the Fjeldly model become apparent. The analytic model, however, still has very good agreement with the TCAD calculation. Finally, when the time scale is shortened to a pulse of a few nanoseconds of duration (Figure 4d), agreement of the analytic model with the TCAD simulation begins to diverge. The excessive sharpness of the analytic solution compared to the TCAD simulation indicates that some of the disagreement is due to the simple method for computing J_{depl}, which assumes an infinite drift velocity. In this device, a carrier takes on the order of 10 ns to traverse the depletion region; that is approximately the same as the pulse width in the 1000× compression case, which indicates the infinite drift velocity assumption is invalid.

V. Conclusion

We presented a new analytic solution that determines the current density coming from an irradiated finite 1D reverse-biased pnn^+ (or npp^+) abrupt junction epitaxial diode. The solution uses the correct nn^+ boundary conditions, as found in [5]. It also improves on the solution in [5] by solving the problem for a finite diode, and taking into account an arbitrary time-dependent radiation generation density. We also developed the analytic solution for a piecewise linear generation function, so that it may be used to analyze realistic pulses—including those based on experimental data. The analytic results compare favorably to TCAD simulations, and represent a substantial improvement over the Fjeldly model [1].

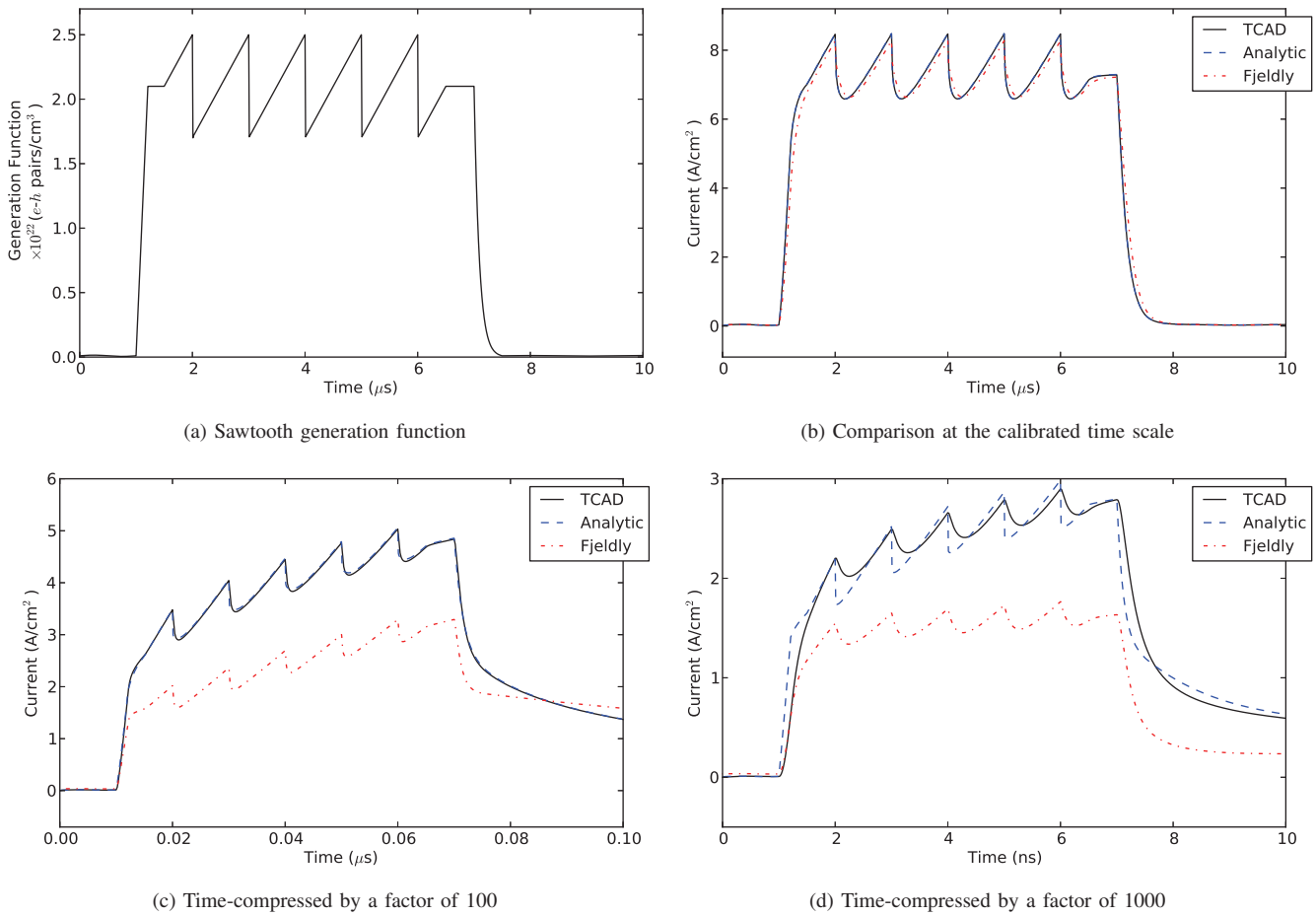

(a) Sawtooth generation function

(b) Comparison at the calibrated time scale

(c) Time-compressed by a factor of 100

(d) Time-compressed by a factor of 1000

Fig. 4. Hypothetical BJT photocurrent comparison, as computed with TCAD, the analytic model, and the Fjeldly model

Finally, we note that the analytic model presented here may also be readily adapted for other applications involving the behavior of excess carriers in undepleted device regions. This includes devices where the generation function has a dependence on both position and time. Examples include optical sensors, photovoltaics and power devices.

ACKNOWLEDGMENT

Sandia National Laboratories is a multi-program laboratory managed and operated by Sandia Corporation, a wholly owned subsidiary of Lockheed Martin Corporation, for the U.S. Department of Energy's National Nuclear Security Administration under contract DE-AC04-94AL85000.

REFERENCES

[1] T. A. Fjeldly, Y. Q. Deng, M. S. Shur, H. P. Hjalmarson, A. Muyshondt, and T. Ytterdal, "Modeling of high-dose-rate transient ionizing radiation effects in bipolar devices," *IEEE Trans. Nucl. Sci.*, vol. 48, no. 5, pp. 1721–1730, 2001.

[2] E. R. Keiter, T. Mei, T. V. Russo, E. L. Rankin, R. L. Schiek, H. K. Thornquist, J. C. Verley, D. A. Fixel, T. S. Coffey, R. P. Pawlowski, K. R. Santarelli, and C. E. Warrender, "Xyce Parallel Electronic Simulator: User's Guide, Version 5.3," Sandia National Laboratories, Albuquerque, NM, Tech. Rep. SAND2012-4085, 2012.

[3] C. L. Axness, B. Kerr, and T. F. Wunsch, "Analytic light - or radiation - induced pn junction photocurrent solutions to the multidimensional ambipolar diffusion equation," *J. Appl. Phys.*, vol. 96, no. 5, pp. 2646–2655, 2004.

[4] J. P. McKelvey, *Solid State and Semiconductor Physics*, Malabar, Florida, 1966.

[5] D. M. Long, J. R. Florian, and R. H. Casey, "Transient response model for epitaxial transistors," *IEEE Trans. Nucl. Sci.*, vol. NS-30, no. 6, pp. 4131–4134, 1983.

[6] C. L. Axness, B. Kerr, and E. R. Keiter, "Analytic 1-D *pn* junction diode photocurrent solutions following ionizing radiation and including time-dependent changes in the carrier lifetime from a nonconcurrent neutron pulse," *IEEE Trans. Nucl. Sci.*, vol. 57, no. 6, pp. 3314 – 3321, 2010.

[7] M. N. Özişik, *Boundary Value Problems of Heat Conduction*. Scranton, PA: International Textbook, 1968.

[8] B. Kerr, C. L. Axness, J. C. Verley, C. E. Hembree, and E. R. Keiter, "A new time-dependent analytic model for radiation-induced photocurrent in finite 1D epitaxial diodes," Sandia National Laboratories, Albuquerque, NM, Tech. Rep. SAND2012-2161, 2012.